ATMOSPHERIC SCIENCE LETTERS
Atmos. Sci. Let. **18**: 261–267 (2017)
Published online 19 May 2017 in Wiley Online Library
(wileyonlinelibrary.com) **DOI:** 10.1002/asl.751

RMetS
Royal Meteorological Society

Projection in snowfall characteristics over the European Alps and its sensitivity to the SST changes: results from a 50 km resolution AGCM

N. Freychet,[1]* H.-H. Hsu,[1] A. Duchez[2] and C.-Y. Tu[1]

[1]*Research Center for Environmental Changes, Academia Sinica, Taipei, Taiwan*
[2]*RAPID Group, National Oceanography Center, Southampton, UK*

**Correspondence to:*
N. Freychet, School of Geosciences, University of Edinburgh, Room 306, Crew Building, The King's Buildings, Alexander Crum Brown Road, Edinburgh EH9 3FF, UK.
E-mail:
nicolas.freychet@gmail.com

Received: 23 September 2016
Revised: 10 February 2017
Accepted: 13 April 2017

Abstract

The end-of-century projection of the snowfall characteristics over the Alps region is studied using the 50-km resolution atmospheric global climate model, HiRAM (high-resolution atmospheric model). The model is forced by three different patterns of projections in the sea surface temperature (SST) in order to assess the sensitivity of snowfall characteristics to theses patterns. It is found that the mean snowfall intensity and frequency is poorly affected by the differences in SST forcing. However, the projections of heavy snowfall events strongly depend on the SST scenario. The changes in temperature and frequency of precipitation and freezing days over the Alps were investigated. We found that these variables did not exhibit a clear dependence to the SST scenario and could not explain the differences observed in snowfall projections. Changes in the moisture transport from the Atlantic Ocean to Europe were found significantly different between each scenario and are assumed to be the main factor affecting the projections of snowfalls, by providing more or less moisture supply.

Keywords: **snow; climate projection; high-resolution atmospheric model; sea surface temperature; HiRAM**

1. Introduction

In a warming climate, snow cover is expected reduce due to a decrease in the number of freezing days and snowfall events and an increase of ablation (Collins *et al.,* 2013) leading to a greater vulnerability of the ecosystem (Kelly and Goulden, 2008; Chen *et al.,* 2011) and the tourism in the Alps (Elsasser and Messerli, 2001). For example, Scherrer *et al.* (2004), using observation, found a reduction of the annual number of snow days at low altitudes (below 1300 m) over the Swiss Alps during the late 20th century. They attributed these changes mainly to changes in the mean temperature, but also pointed out the influence of the North Atlantic Oscillation (NAO) in the South part of the Swiss Alps.

The skill of long-range climate forecasts originate from slowly varying components of the climate system rather than the initial state of the atmosphere, the latter being more important in short-term forecasts (Harrison, 1995; Carson, 1998). One of these low-frequency processes, the sea surface temperature (SST), is predictable months ahead (Barnston *et al.,* 1999), but its long-term projection shows many discrepancies in terms of spatial structure or seasonal signals (Collins *et al.,* 2013). The issue of the SST forcing on weather climate in Europe, particularly in the cold season is important and still not completely understood. An understanding of its effect on snowfall characteristics could enable better adaptation to the change in the risks associated with heavy snowfalls or lack of snow.

Different modelling studies have focused on assessing the impact of climate change on snow cover and extent in different mountains of the world (López-Moreno *et al.*, 2009, 2011; Bavay *et al.,* 2009, 2013; Lafaysse *et al.,* 2014; Piazza *et al.,* 2014). They also assessed the relationship between the SST, surface air temperature and the large-scale atmospheric variability and snow cover over different regions (Ye and Bao, 2001; Scherrer *et al.,* 2004; Hantel and Hirtl-Wielke, 2007; Seager *et al.,* 2010). However, many discrepancies exist among these models, especially in terms of local snow response to different SST forcings (Ma and Xie, 2013).

A current limitation of long-term climate projections is the resolution of the models which can be as coarse as 4° for the CMIP5 model simulations (Taylor *et al.,* 2012) and does not allow a good representation of narrow mountains such as the Alps. Beniston *et al.,* 2003 and Beniston *et al.,* 2011 found that the use of regional climate models (RCMs) can solve this problem, but, because the domain of RCM is limited to a chosen region, this methodology prevents the investigation of the response in snowfall characteristics to remote atmospheric or oceanic forcings (such as SST anomalies) through teleconnections. A statistical downscalling method has also been used (Martin *et al.,* 1996; Castebrunet *et al.,* 2014) but does not resolve explicitly the topographic effect.

A high-resolution atmospheric global climate model (AGCM) is used for the first time in this study, and allows a realistic representation of the Alps topography and the influence of remote teleconnections. Using this high-resolution-coupled model, the aim of this study is to assess how sensible is the projection in snowfall characteristics to different SST forcings. Three different SST patterns of projections are used to investigate their influence on the atmosphere and snowfall characteristics over the Alps. The focus of this study is on the end-of-century projected changes in the characteristics (intensity and frequency) of the snowfall over the Alps, including the mean and most heavy events.

Section 2 describes the data and gives the definition of the investigated variables. Section 3 presents results and Section 4 provides concluding remarks.

2. Data and experiment design

2.1. Model data sets

Daily data from the global high-resolution atmospheric model (HiRAM, Lin, 2004; Putman and Lin, 2007) are used over two periods: 1979–2008 (historical, hereafter HIST) and 2075–2100 (projection, hereafter RCP). The model setup is the same as Chen and Lin, 2012, with a horizontal grid resolution of 50 km corresponding to approximately 0.5° resolution, allowing a good representation of the topography (Figures 1(a) and (b)). The domain covering the Alps is defined in this study as a rectangular box: 6°–16E/43°–49°N (Figure 1(c)).

As illustrated in Figure 2, the largest SST differences are located over the North Atlantic and Arctic regions. C3 (C2) is characterized by a cold (warm) anomaly over the North Atlantic and a weak (strong) increase of temperature over the Arctic, while C1 has a stronger positive anomaly over the North Atlantic but weaker increase over the Arctic. C3 is also characterized by an overall stronger warming of SST over the tropical Atlantic and over the North Sea. Note that there is no significant difference between the three clusters over the Mediterranean Sea, and most of the differences between them are relatively weak (0.5–1 °C) compared to the global mean projected increase in SST [2–3 °C, Figure 2(a)].

Several atmospheric circulation fields are also used to investigate the main dynamical processes: the sea level pressure (SLP), the 850 hPa winds, the 850 hPa atmospheric moisture and the surface temperature to compute the frequency of freezing days. The low-level moisture flux is computed using the winds and moisture and defined as $u \times q$, u being the winds and q the specific humidity.

2.2. Observations

Observations (precipitation and maximum surface air temperature) from the European Gridded Observation (E-OBS) data sets (Haylock *et al.,* 2008) are used for model validation. These observations provide daily outputs at 0.25° resolution and were extracted for the 1979–2008 period (same period as HIST). As there are no snowfall data sets, it is estimated using precipitation and temperature and a snow event is defined as a combination of a positive precipitation and a surface air temperatures equal or below 0°C during the same day. This simple definition is not perfect as snowfall can also occur during days with positive maximum temperatures (leading to a low bias in the estimate) it must be considered with a margin of error.

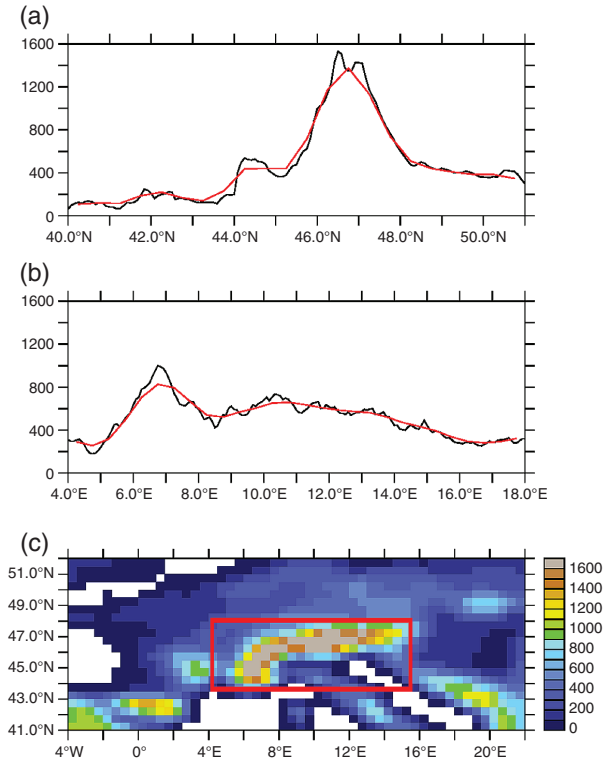

Figure 1. Zonal (a) and meridional (b) averaged topography over the domain defined by the red box on lower caption. The black curve is based on the NOAA NGDC ETOPO5 0.08° topography and the red curve is based on the HiRAM model (0.5° resolution). (c) The model topography and the domain (red box) used for the study.

2.3. Mean and heavy snowfall

Mean and heavy snowfall events are differentiated, and snowfall characteristics are defined by assessing their frequency and intensity.

The mean snowfall intensity is defined as the averaged amount of snow falling per snowing days (expressed in mm day^{-1}). The frequency of mean snowfall corresponds to the number of snowing days per month.

Heavy snowfall is defined as the top 1% most intense snowfall (i.e. the 99th percentile) during the historical period. Intensity and frequency definition of these events is the same that for the mean snowfall but using only heavy snowfall days (i.e. the averaged intensity of snowfall during heavy snowfall days for intensity, and the number of heavy snowfall days per month for the frequency).

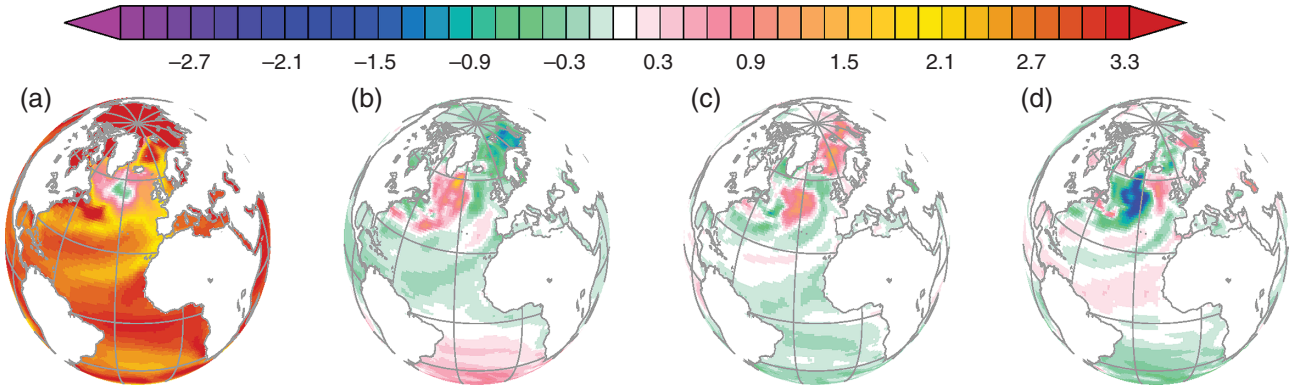

Figure 2. (a) HiRAM ensemble mean (i.e. average of C1, C2 and C3) change in SST during DJF between HIST and RCP periods (°K). (b–d) Differences between the changes in C1, C2 and C3 SST and the ensemble mean change (i.e. C1-mean, C2-mean and C3-mean).

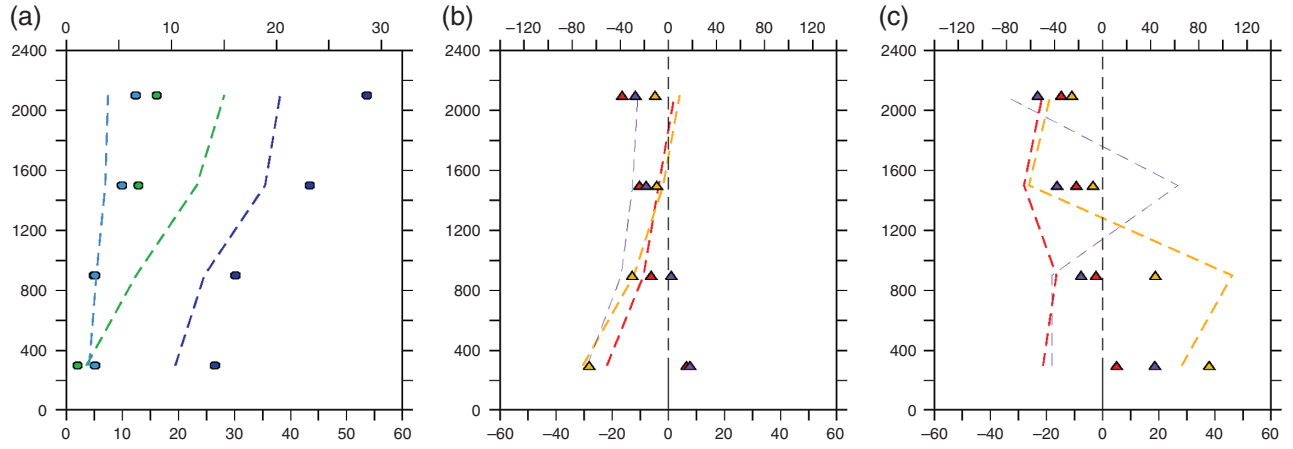

Figure 3. Snowfall characteristics averaged over the Alps region (6°–16°E, 42°–49°N) and every 600 m elevation. (a) Mean (light blue) and heavy (dark blue) snowfall intensity (mm day^{-1}, bottom scale), from observation (circle symbols) and HiRAM model (dashed lines). Green symbols indicate the frequency of the snow events (day month^{-1}, top scale). (b) Changes for each member (C1: red; C2: orange; C3: purple) of the mean snowfall intensity (shaded triangles, percentage, bottom scale) and frequency (dashed lines, percentage, upper scale). (c) Same as (b) but for the heavy snowfall events.

All the values are computed for each grid point, and then eventually averaged over time and space to display the results.

3. Change in snowfall characteristics: sensitivity to the SST forcing

3.1. Historical run evaluation

First, a quick evaluation of the model simulations used in this study is conducted for the HIST run and illustrated in Figure 3(a). The intensity and frequency of the mean and heavy snowfalls are averaged over 600-m elevation bands, based on the model topography.

HiRAM can adequately represent the profiles of mean and heavy snowfall intensity (light and dark blue), although these intensities are underestimated in the high altitudes (above 1200 m). At these elevations, the model displays a larger frequency of snow events (green), but as said before, this might also be due to the way snow events are defined in the observations.

3.2. Elevation dependence

Output from each RCP projection are analysed in Figure 3(b). For all three members, a diminution in the frequency of mean snow events is observed compared to HIST, especially at altitudes below 600 m (40–80% reduction). The mean intensity is also projected to reduce for each member, except at the lowest elevation, where C1 and C3 show a slight increase in the intensity (+7%), while C2 exhibit the strongest decrease (−30%).

This difference in behaviour at low elevation between C2 and the other members is also visible when looking at the heavy event signals (Figure 3(c)). C2 is the only case that shows a clear increase in both intensity and frequency of heavy snowfalls below 1200 m (up to +40% and +110%, respectively). At higher elevation (above 1200 m), both intensity and frequency decrease. The two other members agree on an increase of the intensity of heavy events at the lowest elevation, but both show a decrease in frequency.

The most significant impact of the SST scenario forcing on snowfall projections is thus at lower elevation

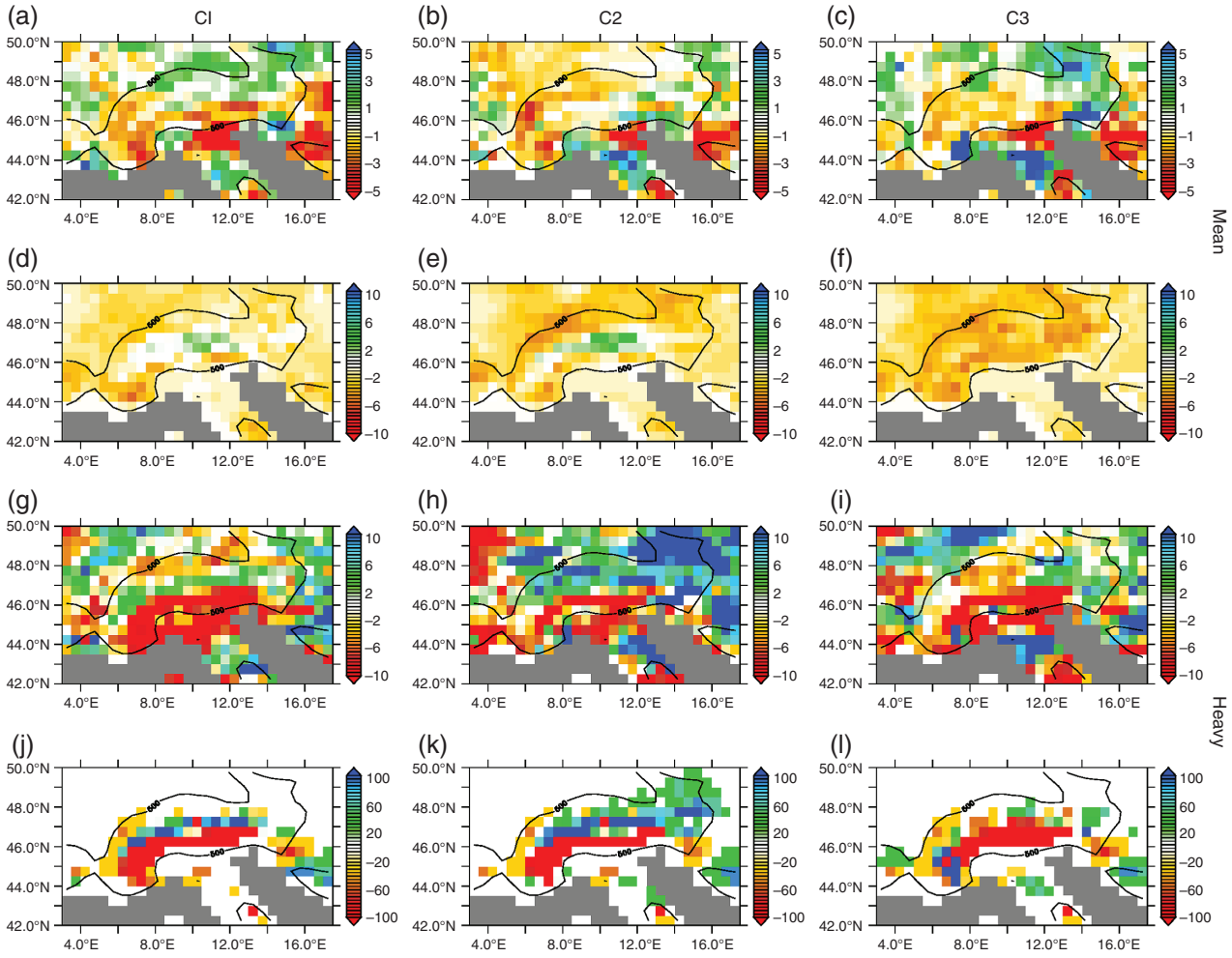

Figure 4. Change, for each member, in mean snowfall intensity (a–c, mm day^{-1}) and frequency (d–f, day month^{-1}). (g–l) Same as (a–f) but for heavy snowfall except that (j–l) are expressed in percentage. The black contour highlights the 500 m altitude contour, based on the model topography.

(below 1200 m), especially for heavy events. At higher altitude, the tendencies in each member are similar and less dependent on the SST scenario. As snowfalls are closely related to the atmospheric temperature, the projections of the number of freezing days (i.e. with a surface air temperature below 0 °C) is also investigated for each altitude band (not shown). No significant differences were found between the members, each of them exhibiting a reduction in freezing days at all elevations but with a stronger signal below 1200 m. Thus, the differences in the projected snowfall characteristics are not due to changes in surface temperature, but could be attributed to other factors such as the large-scale atmospheric circulation and moisture supply. These hypotheses are investigated in Section 3.4.

3.3. Spatial asymmetry of the changes

The spatial patterns of mean and heavy snowfall characteristics associated with each RCP simulation are now analysed. Figure 4 displays the projected changes (RCP-HIST) for each case.

In terms of mean snowfall intensity (Figures 4(a)–(c)) of all members tend to show a dipole pattern, with a decrease over the southern and western part of the domain and an increased intensity over the northern and eastern parts of the Alps. The magnitude of these changes differs for each case, with C1 (C3) having a more intense signal over the South (East) and C2 showing a larger but less intense decrease over the northern and western part of the Alps.

In terms of mean snowfall frequency (Figures 4(d)–(f)), C3 indicates a reduction in the number of snow events everywhere while C1 and C2 show a weak increase in the centre of the Alps (the highest parts), which is consistent with results from the previous section (Figure 3(b)). This point illustrates the importance to have a resolution high enough to explicitly resolve the topography effects, even in terms of climate projections.

Heavy snowfall projections show even clearer differences between the three members (Figures 4(g)–(l)). In terms of intensity (g–i), C2 is characterized by a clear and strong increase almost everywhere except over the southern regions, while C1 and C3 show an overall decrease except in the eastern-central part of the mountains. The frequency (j–l) has similar signals, with C2 showing a strong increase over the central

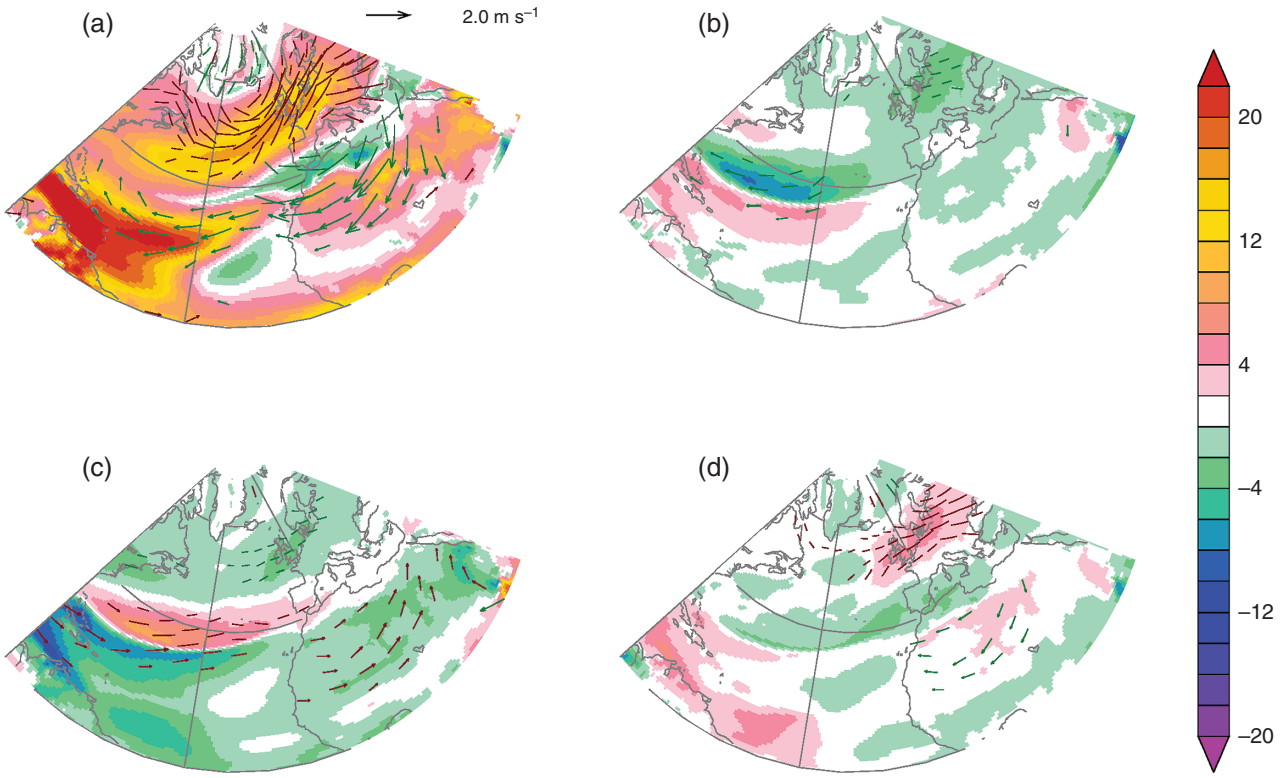

Figure 5. (a) Ensemble mean change (during DJF) of the 850 hPa moisture flux MF ($g\,kg^{-1}.m^{-1}\,s^{-1}$, shading) and 850 hPa wind (vectors) between RCP and HIST period. (b–d) Difference between the change of moisture flux (MF) and wind for each member compared to the ensemble mean change. For the winds, green (red) vectors indicate a westward (eastward) anomaly.

and northern parts of the Alps while the other members exhibit mostly a decrease, except C1 over the central band.

Once again, the impact of the topography is undeniable, with a clear meridional transition of the patterns along the centre of the Alps. The sensibility of the heavy snowfall projections to the SST scenario is also clear, especially over the northern part of the Alps.

The above results indicate that spatial patterns of projected changes in snow characteristics are closely linked to the SST forcing patterns. An analysis of the spatial changes in surface temperature and number of freezing days (not shown) did not show significant differences between the members. All projections indicate a large increase in the temperature over the Alps (up to 4 °C) and a decrease of the number of freezing days everywhere (a decrease of 3–5 days per month in the Alps). Thus, the SST patterns do not affect directly the projected changes in the temperature, and the observed differences in the snowfall characteristics may be due to other factors, investigated in the next section.

3.4. Possible influence of large-scale atmospheric circulation

Winter European climate is strongly related to the atmospheric circulation over the North Atlantic and its first mode of variability is often characterized by the NAO index, as shown by Heaps *et al.,* 2013, for example. In this section, the RCP projections of the circulation are investigated for each SST forcing to highlight the differences and to find the possible explanations of the snowfall sensitivity.

The mean RCP projected change (i.e. the averaging of C1, C2 and C3, minus HIST) in the winter large-scale atmospheric circulation (850 hPa wind and moisture transport, MT) is displayed in Figure 5(a). The differences between each member (C1, C2 and C3) and the mean projection are displayed in the same figure (b–d). The mean change looks like a typical NAO+ circulation pattern, with an increased MT from the ocean to the northern part of Europe and a decrease over the Mediterranean region. It is related to a large increase in SLP over the South of Europe and a decrease over the Arctic region (not shown).

The signal in C2 is sensibly different from the mean, with a stronger MT reaching the South of Europe due to a weaker increase in the SLP over the Mediterranean region. On the opposite, in C3 the MT is even more deviated to the northern part of Europe and Scandinavia, which is typically associated with a cold blob over the North Atlantic (Duchez *et al.,* 2016). In C1, the overall MT is reduced. These differences are associated with a large increase in the specific humidity over the Alps in C2 compared with the two other cases (not shown). C3 has the strongest NAO type signal, but, because the MT is deviated too much to the North, the Alps region are drier. The signal in C1 is less intense and thus the possible impact on the snowfall is less clear.

It is assumed that these differences in the MT are the main factors that can explain the differences in the projections of heavy snowfall for C2. Indeed, a difference in the atmospheric moisture supply could explain why in C2, heavy snowfall is enhanced. However, this is a sensible result. All three members show a NAO+-like projection, and the differences between each case are moderate. But, it is enough to lead to large differences in the snowfall projections and it is clear that heavy snowfall projections are sensible to the characteristic of the circulation over the North Atlantic and to the patterns of the SST.

4. Discussion and conclusion

The aim of this study is to assess the sensibility of the RCP climate projection in snowfall over the Alps to three different SST forcings, using a global HiRAM.

The experiments reveal both consistency and differences in the RCP projections of the snowfall characteristics between each case. The number of snowfall days is projected to reduce in all cases, due to an increase in the surface temperature and a decrease in the number of freezing days. This signal is consistent between all members. Changes in heavy snowfall characteristics are sensitive to the detailed structure of the projected SST patterns. One case (C2) exhibits a particularly strong increase (in both frequency and intensity) at low elevations (below 1200 m) and over a large region (central and northern part of the Alps). The differences may be related to the moisture transport from the North Atlantic. Indeed, in C2 the moisture transport is stronger over the southern part of Europe compared with the other cases. Thus, even if the patterns of the SST change do not strongly impact the projections of the mean snowfall, they could be important for local or regional projections of heavy rainfall.

Acknowledgements

This work was supported by the Consortium for Climate Change Study (CCliCS) – Ministry of Science and Technology (MOST), Taiwan, under Grant MOST 105-2119-M-001-018. We thank the reviewers for comments that greatly improved the manuscript.

References

Barnston AG, He Y, Glantz MH. 1999. Predictive skill of statistical and dynamical climate models in SST forecasts during the 1997–98 El Niño episode and the 1998 La Niña onset. *Bull. Am. Meteorol. Soc.* **80**(2): 217–243.

Bavay M, Lehning M, Jonas T, Loewe H. 2009. Simulations of future snow cover and discharge in Alpine headwaters catchments. *Hydrological Processes* **23**: 95–108.

Bavay M, Grünewald T, Lehning M. 2013. Response of snow cover and runoff to climate change in high Alpine catchments of Eastern Switzerland. *Advances in Water Resources* **55**: 4–16. https://doi.org/10.1016/j.advwatres.2012.12.009.

Beniston M, Kelle F, Koffi B, Goyette S. 2003. Estimates of snow accumulation and volume in the Swiss Alps under changing climatic conditions. *Theoretical and Applied Climatology* **76**(3-4): 125–140.

Beniston M, Uhlmann B, Goyette D, Lopez-Moreno JI. 2011. Will snow-abundant winters still exist in the Swiss Alps in an enhanced greenhouse climate? *International Journal of Climatology* **31**: 1257–1263. https://doi.org/10.1002/joc.2151.

Carson DJ. 1998. Seasonal forecasting. *Q. J. R. Meteorol. Soc.* **124**(545): 1–26.

Castebrunet H, Eckert N, Giraud G, Durand Y, Morin S. 2014. Projected changes of snow conditions and avalanche activity in a warming climate: the French Alps over the 2020–2050 and 2070–2100 periods. *The Cryosphere* **8**(5): 1673–1697.

Chen JH, Lin SJ. 2012. Seasonal prediction of tropical cyclones using a 25-km resolution general circulation model. *Journal of Climate* **26**: 380–398.

Chen IC, Hill JK, Ohlemüller R, Roy DB, Thomas CD. 2011. Rapid range shifts of species associated with high levels of climate warming. *Science* **333**(6045): 1024–1026.

Collins M, Knutti R, Arblaster J, Dufresne JL, Fichefet T, Friedlingstein P, Gao X, Gutowski WJ, Johns T, Krinner G, Shongwe M, Tebaldi C, Weaver AJ, Wehner M. 2013. Longterm Climate Change: Projections, Commitments and Irreversibility. In *Climate Change 2013: The Physical Science Basis*, Stocker TF, Qin D, Plattner G-K, Tignor M, Allen SK, Boschung J, Nauels A, Xia Y, Bex V, Midgley PM (eds). Contribution of Working Group I to the Fifth Assessment Report of the Intergovernmental Panel on Climate Change. Cambridge University Press: Cambridge; New York, NY.

Duchez A, Frajka-Williams E, Josey SA, Evans DG, Grist JP, Marsh R, McCarthy GD, Sinha B, Berry DI, Hirschi JJM. 2016. Drivers of exceptionally cold North Atlantic Ocean temperatures and their link to the 2015 European heat wave. *Environmental Research Letters* **11**(7): 074004.

Elsasser H, Messerli P. 2001. The vulnerability of the snow industry in the Swiss Alps. *Mountain Research and Development* **21**(4): 335–339. https://doi.org/10.1659/0276-4741(2001)021[0335:TVOTSI]2.0.CO;2.

Hantel M, Hirtl-Wielke LM. 2007. Sensitivity of Alpine snow cover to European temperature. *International Journal of Climatology* **27**: 1265–1275. https://doi.org/10.1002/joc.1472.

Harrison MSJ. 1995. Long-range forecasting since 1980: Empirical and numerical prediction out to one month for the United Kingdom. *Weather* **50**(12): 440–449.

Haylock MR, Hofstra N, Klein Tank AMG, Klok EJ, Jones PD, New M. 2008. A European daily high-resolution gridded data set of surface temperature and precipitation for 1950–2006. *Journal of Geophysical Research: Atmospheres* **113**: D20119. https://doi.org/10.1029/2008JD010201.

Heaps R, Hirschi J, Sinha B. 2013. Weather asymmetric response of European pressure and temperature anomalies to NAO positive and NAO negative winters. *Weather* **68**(3): 73–80.

Kelly AE, Goulden ML. 2008. Rapid shifts in plant distribution with recent climate change. *Proceedings of the National Academy of Sciences of the United States of America* **105**(33): 11823–11826.

Lafaysse M, Hingray B, Mezghani A, Gailhard J, Terray L. 2014. Internal variability and model uncertainty components in future hydrometeorological projections: The Alpine Durance basin. *Water Resources Research* **50**: 3317–3341. https://doi.org/10.1002/2013WR014897.

Lin SJ. 2004. A vertically Lagrangian finite-volume dynamical core for global models. *Monthly Weather Review* **132**: 2293–2307.

López-Moreno JI, Goyette S, Beniston M. 2009. Impact of climate change on snowpack in the Pyrenees: horizontal spatial variability and vertical gradients. *Journal of Hydrology* **374**: 384–396.

López-Moreno JI, Goyette S, Vicente-Serrano SM, Beniston M. 2011. Effects of climate change on the intensity and frequency of heavy snowfall events in the Pyrenees. *Climatic Change* **105**: 489–508.

Ma J, Xie SP. 2013. Regional patterns of sea surface temperature change: a source of uncertainty in future projections of precipitation and atmospheric circulation. *Journal of Climate* **26**(8): 2482–2501.

Martin E, Timbal B, Brun E. 1996. Downscaling of general circulation model outputs: simulation of the snow climatology of the French Alps and sensitivity to climate change. *Climate Dynamics* **13**: 45–56.

Piazza M, Boé J, Terray L, Pagé C, Sanchez-Gomez E, Dequé M. 2014. Projected 21st century snowfall changes over the French Alps and related uncertainties. *Climatic Change* **122**: 583–594. https://doi.org/10.1007/s10584-013-1017-8.

Putman WM, Lin SJ. 2007. Finite-volume transport on various cubed-sphere grids. *Journal of Computational Physics* **227**: 55–78.

Scherrer SC, Appenzeller C, Laternser M. 2004. Trends in Swiss Alpine snow days: the role of local- and large-scale climate variability. *Geophysical Research Letters* **31**: L13215. https://doi.org/10.1029/2004GL020255.

Seager R, Naik N, Vecchi GA. 2010. Thermodynamic and dynamic mechanisms for large-scale changes in the hydrological cycle in response to global warming. *J. Clim*. **23**(17): 4651–4668.

Taylor KE, Stouffer RJ, Meehl GA. 2012. An overview of CMIP5 and the experiment design. *Bulletin of the American Meteorological Society* **93**(4): 485.

Ye H, Bao Z. 2001. Lagged teleconnections between snow depth in northern Eurasia, rainfall in Southeast Asia and sea-surface temperatures over the tropical Pacific Ocean. *Int. J. Climatol*. **21**(13): 1607–1621.